crystallization papers

Crystallization and preliminary X-ray analysis of sulfite dehydrogenase from *Starkeya novella*

Ulrike Kappler[a] and Susan Bailey[b]*

[a]University of Queensland, St Lucia, Qld 4072, Australia, and [b]CCLRC Daresbury Laboratory, Warrington WA4 4AD, England

Correspondence e-mail: s.bailey@dl.ac.uk

Crystals of purified heterodimeric sulfite dehydrogenase from *Starkeya novella* have been grown using vapour diffusion. X-ray diffraction data have been collected from crystals of the native protein at $\lambda = 1.0$ Å and close to the iron absorption edge at $\lambda = 1.737$ Å. The crystals belong to space group $P2_12_12$, with unit-cell parameters $a = 97.5$, $b = 92.5$, $c = 55.9$ Å. Native data have been recorded to 1.8 Å resolution and Fe-edge data to 2.5 Å.

1. Introduction

Sulfite-oxidizing enzymes that convert the highly reactive and therefore toxic sulfite to sulfate have been identified in insects, animals, plants and bacteria (Enemark *et al.*, 2003; Enemark & Cosper, 2002; Kisker *et al.*, 1997; Rajagopalan, 1980; Schrader *et al.*, 2003). While the well studied enzymes from higher animals serve to detoxify sulfite that arises from the catabolism of sulfur-containing amino acids, the bacterial enzymes have a central role in converting sulfite formed during dissimilatory oxidation of reduced sulfur compounds (Kappler & Dahl, 2001). Only one of these enzymes, the sulfite dehydrogenase from the soil bacterium *Starkeya novella*, has been purified to homogeneity and studied in some detail to date (Aguey-Zinsou *et al.*, 2003; Feng *et al.*, 2003; Kappler *et al.*, 2000, 2001). The enzyme contains 454 amino acids and has a molecular weight of 49 000 Da. Unlike the homodimeric Mo- and haem *b*-containing sulfite oxidases found in higher animals, this enzyme is a heterodimer comprising a 373-residue molybdopterin cofactor (Moco) subunit (SorA) and a smaller 81-residue haem *c* subunit (SorB). In addition, the sulfite dehydrogenase can only transfer electrons to cytochrome *c*, its natural electron acceptor, or ferricyanide and does not react with molecular oxygen, which can serve as an electron acceptor for sulfite oxidases (Kappler & Dahl, 2001). The crystal structures of two sulfite oxidases, one from chicken liver (Kisker *et al.*, 1997) and the other from the plant *Arabidopsis thaliana* (Schrader *et al.*, 2003), have been reported previously. Chicken sulfite oxidase (CSO) is a homodimer with a total molecular weight of approximately 100 kDa, with each subunit comprising three domains: an N-terminal haem *b* domain, a Moco-containing domain and a C-terminal dimerization domain.

The plant enzyme (PSO) is also a homodimer, but unlike CSO each subunit comprises only two domains; there is no haem domain. The known protein sequences of eukaryotic sulfite oxidases share between 39 and 77% identity. Comparison with bacterial sulfite dehydrogenases reveals a lower level of sequence identity of around 30%. Specifically, SorA has a primary sequence identity of 32% and 30% with the Moco and dimerization domains of CSO and PSO, respectively. Given the structural differences of the bacterial sulfite dehydrogenase and the sulfite oxidases, a crystal structure for this enzyme will significantly enhance our understanding of the molecular mechanisms underlying enzymatic sulfite oxidation.

2. Experimental procedure and results

2.1. Protein expression and purification

Recombinant SorAB (rSorAB) was expressed in *Rhodobacter capsulatus* 37B4 $\Delta dorA$ strain following the previously described method (Kappler & McEwan, 2002). Briefly, *R. capsulatus* cells transformed with the pRK-sorex plasmid were grown phototrophically for 18–20 h on RCV supplemented with tetracycline (1 µg ml^{-1}), 60 mM dimethyl sulfoxide and 1 mM sodium molybdate. The cells were harvested by centrifugation and periplasmic extracts were prepared which were loaded onto a DEAE-Sephacel column equilibrated with 20 mM Tris–HCl pH 7.8 (buffer A). A linear gradient of buffer A plus 1–250 mM NaCl was used to wash the protein from the column. Active fractions were concentrated and solid ammonium sulfate was added to a concentration of 15%(w/v). The sample was applied onto a phenyl Sepharose FF column equilibrated with 15% ammonium sulfate in buffer A. rSorAB was eluted with a

step gradient, reducing the ammonium sulfate concentration to 11.5%. The sample was dialysed against buffer *A* with 150 m*M* NaCl, concentrated and further purified by size-exclusion chromatography on a Hi-Load Superdex75 column.

After the size-exclusion step, the purity of the protein was confirmed by SDS–PAGE, yielding two bands at apparent molecular weights of 40 000 and 8 000 Da, which correspond to the SorA molybdoprotein and the SorB cytochrome *c* subunit of the heterodimer, respectively. The final protein concentration was estimated from the absorbance at 280 nm using a measured coefficient of 60.214 mM^{-1} cm^{-1} (U. Kappler, unpublished data).

2.2. Crystallization

The purified protein is typically a mixture of oxidized and reduced forms. As the protein does not transfer electrons to molecular oxygen, both forms are very stable. Reduction of the protein with sulfite appears to cause conformational changes that result in a higher temperature stability of the protein (inactivation: SorAB ox, >333 K; SorAB red, >343 K). Prior to crystallization, the protein was buffer-exchanged into a solution of 10 m*M* Tris–HCl pH 8 and 2 m*M* sodium sulfite was added to reduce the protein.

Initial screening for nucleation and crystallization conditions was performed using sitting-drop vapour diffusion at 294 and 278 K. Suitable conditions were identified using reduced protein and the commercially available Hampton Crystal Screens I and II. In all cases, the drops were prepared by the addition of 3 µl of the reservoir solution to 3 µl protein solution at 10 mg ml^{-1}. The droplets were equilibrated against a reservoir volume of 0.5–1.0 ml in 24-well

Figure 1
Clump of crystals of sulfite-reduced sulfite dehydrogenase. The largest individual crystal plates are approximately 20 × 500 × 500 µm.

Cryschem crystallization plates. Crystals appeared in several drops in plates incubated at 294 K. Two of these conditions were optimized for reproducible production of crystals and the crystals were tested for diffraction. The best conditions used vapour diffusion against a solution of 100 m*M* HEPES pH 7.4, 2.2 *M* ammonium sulfate and 2%(*v/v*) PEG 200 and yielded crystals that diffracted well and were stable over a period of weeks. The crystals typically grew as clumps of very thin plates as shown in Fig. 1; attempts to improve the morphology of the crystals were unsuccessful. Crystals of the oxidized protein could be obtained using the same conditions except that 1 m*M* potassium ferricyanide was added to oxidize the protein prior to setting up the crystallization experiments.

2.3. Data collection and processing

In order to collect data, it was necessary to break off a fragment of a single plate, which would typically be of dimensions 10–20 × 200 × 200 µm. Although the plates are thin, the crystals diffract to at least 1.8 Å using synchrotron radiation. All data collection described in this paper used crystals obtained from protein reduced by the addition of 2 m*M* sulfite. Prior to cooling, the crystals were cryoprotected by the addition of approximately 20%(*v/v*) glycerol. The crystals were then mounted in loops and flash-cooled either by dipping in liquid nitrogen or by exposure to a cryostream. X-ray diffraction data were measured using synchrotron radiation at 100 K. Data were collected at beamline 8.2.2 with a 315 mm ADSC CCD detector at the Advanced Light Source, Lawrence Berkeley National Laboratory, CA, USA with an exposure time of 30 s and a 1° oscillation angle.

Table 1 details the data-collection parameters. The potential space group and unit-cell parameters were determined and the reflection intensities were measured using the program *MOSFLM* (Leslie, 1992). Intensity data were scaled using the *CCP*4 program *SCALA* (Collaborative Computational Project, Number 4, 1994). The data are consistent with space group $P2_12_12$ and the unit-cell parameters were determined to be *a* = 97.5, *b* = 92.5, *c* = 55.9 Å. Native crystals were used for data collection using X-radiation at λ = 1.0 Å, providing native 1.8 Å resolution data. A fluorescence scan of the iron absorption edge was very noisy and the exact position of the edge was not clear, so we chose to collect a data set to 2.5 Å resolution at λ = 1.737 Å on the high-energy

Table 1
Data-collection and processing statistics.

Values in parentheses refer to the highest resolution shell (1.90–1.80 Å for the native data and 2.64–2.5 Å for the Fe-edge data).

	Native I	Fe edge
Beamline	ALS BL8.2.2	ALS BL8.2.2
No. images	180	130
Temperature (K)	100	100
Wavelength (Å)	1.0	1.737
Resolution range (Å)	17–1.8	67–2.5
Total observations	259001	67132
Unique reflections	45440	17778
Completeness (%)	95.6 (77.5)	97.7 (96.7)
Multiplicity	5.7 (3.0)	3.8 (3.6)
$I/\sigma(I)$	20.8 (5.7)	13.4 (6.4)
R_{merge} (%)	6.5 (19.3)	8.7 (17.8)

† $R_{merge} = \sum_h \sum_i |I_{hi} - I_h| / \sum_h \sum_i I_{hi}$.

side of the Fe edge. Assuming the presence of one molecule in the asymmetric unit, the crystal volume per unit molecular weight is 2.6 Å^3 Da^{-1} (Matthews, 1968) and indicates a solvent content of around 50%.

Molecular replacement was attempted using the programs *MOLREP* (Vagin & Teplyakov, 1997) and *BEAST* (Read, 2001) using CSO as a search model (Kisker *et al.*, 1997). CSO has a primary sequence identity with SorA of 32% for the Moco and dimerization domains, residues 92–453, which comprise 90% of the protein. The N-terminal domain of CSO, corresponding to a cytochrome b_5 domain, was excluded from the search model. Trials at varying resolutions and with both programs gave very similar solutions using the Moco and dimerization domains together or the Moco domain on its own (residues 106–308, 34% sequence identity). The highest correlation was obtained using only the Moco domain and when side chains in the search model were truncated to atoms common to both CSO and SorAB. However, these solutions could not be successfully used as the starting point for refinement and calculated $(2F_o - F_c)$ and $(F_o - F_c)$ maps were not interpretable. Difference Fourier maps calculated using the phases from MR solution together with the anomalous differences from the Fe-edge data did not identify the Fe site of SorB, the cytochrome *c* subunit. Determination of the Fe position using the Fe-edge data was attempted with the programs *SHELXD* and *SOLVE* but did not yield a significant site. This may be because of the effects of radiation damage, which were apparent towards the end of data collection at the longer wavelength. The crystals have been soaked in a variety of heavy-atom solutions and investigations of possible heavy-atom derivatives are under way.
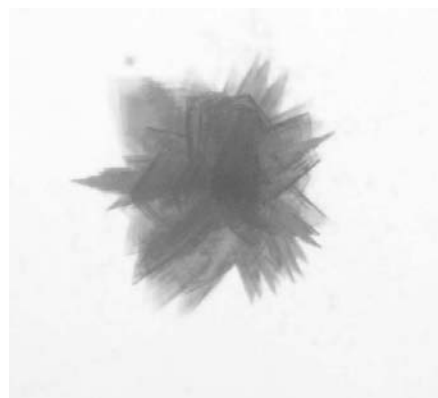
crystallization papers

References

Aguey-Zinsou, K. F., Bernhardt, P. V., Kappler, U. & McEwan, A. G. (2003). *J. Am. Chem. Soc.* **125**, 530–535.

Collaborative Computational Project, Number 4 (1994). *Acta Cryst.* D**50**, 760–763.

Enemark, J. H., Astashkin, A. V. & Raitsimring, A. M. (2003). *ACS Symp. Ser.* **858**, 179–192.

Enemark, J. H. & Cosper, M. M. (2002). *Met. Ions Biol. Syst.* **39**, 621–654.

Feng, C. J., Kappler, U., Tollin, G. & Enemark, J. E. (2003). *J. Am. Chem. Soc.* **125**, 14696–14697.

Kappler, U., Bennett, B., Rethmeier, J., Schwarz, G., Deutzmann, R., McEwan, A. G. & Dahl, C. (2000). *J. Biol. Chem.* **275**, 13202–13212.

Kappler, U. & Dahl, C. (2001). *FEMS Microbiol. Lett.* **203**, 1–9.

Kappler, U., Friedrich, C. G., Truper, H. G. & Dahl, C. (2001). *Arch. Microbiol.* **175**, 102–111.

Kappler, U. & McEwan, A. G. (2002). *FEBS Lett.* **529**, 208–214.

Kisker, C., Schindelin, H., Pacheco, A., Wehbi, W. A., Garrett, R. M., Rajagopalan, K. V.,

Enemark, J. H. & Rees, D. C. (1997). *Cell*, **91**, 973–983.

Leslie, A. G. W. (1992). *Jnt CCP4/ESF–EACMB Newsl. Protein Crystallogr.* **26**.

Matthews, B. W. (1968). *J. Mol. Biol.* **33**, 491–497.

Rajagopalan, K. V. (1980). *Molybdenum- and Tungsten-Containing Enzymes*, edited by M. P. Coughlan, pp. 243–272. Oxford: Pergamon Press.

Read, R. J. (2001). *Acta Cryst.* D**57**, 1373–1382.

Schrader, N., Fischer, K., Theis, K., Mendel, R. R., Schwarz, G. & Kisker, C. (2003). *Structure*, **11**, 1251–1263.

Vagin, A. & Teplyakov, A. (1997). *J. Appl. Cryst.* **30**, 1022–1025.